Available online at www.sciencedirect.com
ScienceDirect
Nuclear Instruments and Methods in Physics Research A 579 (2007) 782–787
NUCLEAR INSTRUMENTS & METHODS IN PHYSICS RESEARCH Section A
www.elsevier.com/locate/nima

Systematic study of micro-discharge characteristics of ATLAS barrel silicon microstrip modules

T. Kuwano[a], K. Hara[a,*], S. Shinma[a], Y. Ikegami[b], T. Kohriki[b], S. Terada[b], Y. Unno[b]

[a]*Institute of Pure and Applied Sciences, University of Tsukuba, 1-1-1 Ten'nodai, Tsukuba, Ibaraki 305-8571, Japan*
[b]*High Energy Accelerator Research Organization (KEK), Oho 1-1, Tsukuba, Ibaraki 305-0801, Japan*

Available online 31 May 2007

Abstract

Among the 981 silicon microstrip modules fabricated by the ATLAS SCT Japan group, 111 modules showed a micro-discharge, a rapid leakage current increase when the bias is raised, below 500 V bias at least once in the series of the quality assurance testing. We have conducted a systematic study to understand the causes, including the hot spot localization using an infrared sensitive camera, and measurement of leakage current decay time.

PACS: 29.40.Gx; 29.40.Wk

Keywords: Silicon microstrip; ATLAS; SCT; Micro-discharge; Hot electron

1. Introduction

The ATLAS Detector is under construction for the LHC Collider Experiment to reveal the origin of the mass and to explore new physics in the regime provided by proton–proton collisions at 14 TeV center-of-mass energy. The Semiconductor Tracker (SCT) [1] based on a technology of silicon microstrips is one of the three ATLAS Inner Tracking systems, PIXEL Tracker, SCT and Transition Radiation Tracker, located inside a 2 T magnetic field. The SCT consists of four concentric barrels in the central region, $30 < r < 60$ cm and $|z| < 80$ cm, and nine discs each in the forward/backward regions, $80 < |z| < 270$ cm, where r is the radial distance and z is the distance along the beam pipe from the collision point. The barrels are constructed from 2112 silicon microstrip modules that are identical in design. Each barrel module has four single-sided microstrip sensors, glued back-to-back on to a baseboard. The dimensions of the silicon sensors are 63.56×63.96 mm with a thickness of 290 μm. The strips of the two sensors on the same side of a module are wirebonded together, with a stereo angle of 40 mrad subtended between the top and bottom strips.

All the silicon sensors for the barrel modules were fabricated by Hamamatsu Photonics (HPK) using 4″ process technology. There are 768 readout strips per sensor at a pitch of 80 μm. The 16 μm wide p^+ implant electrodes are biased through poly-silicon resistors of 1.5 MΩ. The 22 μm wide readout Al electrodes are AC coupled via SiO_2 and Si_3N_4 layers. The overhang design of Al electrodes over the implants moves the high edge electric field from the silicon into the oxide layer, hence reducing the risk of electrical breakdown.

The barrel modules were constructed at four qualified construction sites where thorough quality assurance was carried out based on an agreed program. The program included metrology measurements, thermal cycling tests, electrical tests at −15 and 15 °C where the test pulse system incorporated in the ABCD3T [2] chips characterized the defective channels, and *IV* scans.

The *IV*, leakage current vs. bias voltage, characterization is one of the critical test procedures. Among the 981 barrel modules constructed at the Japanese site, 111 modules showed a rapid leakage current increase at a bias voltage below 500 V. Such a rapid current increase can be

*Corresponding author.
E-mail address: hara@hep.px.tsukuba.ac.jp (K. Hara).

0168-9002/$ - see front matter © 2007 Elsevier B.V. All rights reserved.
doi:10.1016/j.nima.2007.05.288

explained by a micro-discharge [3]. The drifting carriers are accelerated by the local high electric field, and generate multiple secondary electron-hole pairs, resulting in a rapid leakage current increase. The local high field is often created in the vicinity of the strips where the field is maximal and any existing defects increase the field further. Infrared radiation associated to the multiplication process could be viewed with an infrared sensitive (IR) camera as a hot spot, which can help localizing the micro-discharge.

We have carried out a series of systematic measurements to characterize the properties of the 111 modules which exhibited a degraded *IV* curve. For such modules, the SCT module community required to derive the decay time of the leakage current when the module is kept at 500 V bias. In addition to this test, the Japanese Group tried to localize the hot spot with an IR camera and to identify any associated visible traces. The noise distribution available from the electrical tests was also utilized to compare with the visual and IR information. The sensor leakage current specification to the manufacturer was defined in the bias range below 350 V, while we extended the maximum bias up to 500 V after the contract had been placed. Therefore some sensors accepted at delivery showed the micro-discharge in the extended bias region. Because of this and of the fact that HPK can produce sensors with superior *IV* characteristics with the 6″ process [4], the present study provides limited information only specific to our case, the fraction of micro-discharge sensors, for example. Nevertheless, the systematic study presented here covers general micro-discharge properties. The results should be useful to understand its origin, and hence suppress micro-discharge occurrence in future sensor manufacturing.

2. *IV* and hot spot measurement procedures

2.1. *IV* measurements

The requirement to the leakage current per sensor is less than 2 μA at 350 V when the current is scaled to 20 °C. The *IV* per sensor was scanned at about 25° room temperature and 50% relative humidity by HPK. For most of the sensors the leakage current was less than 0.2 μA with a distribution peaking around 0.13 μA at 350 V. The sensors were *IV* re-tested up to 500 V before they were assembled into modules. The sensors, which showed substantially larger currents were grouped and used in the same module so that the number of modules exhibiting micro-discharge is kept small.

The module *IV* scan is a part of the agreed electrical test procedure. The measurement took place at least four times before module shipment. The first module *IV* scan was taken at 15 °C and 50% relative humidity at the module construction sites, HPK and Seiko Precision Inc. (SPI). The other *IV* tests were performed at KEK once at −16 °C and twice at 15 °C. At KEK, up to 12 modules were tested together in a light-tight thermostat chamber flushed with dry N_2. The leakage current was measured up to 500 V with a step of 10 or 15 V. The current was read out 10 s after the bias was stepped up.

In order to examine the dependence of the micro-discharge onset voltage on humidity and temperature, we have conducted the following tests. First, we compared the micro-discharge onset voltages for 15 modules at 0% and 50% relative humidity. All the onset voltages, typically 450 V at 0% humidity, shifted upwards at 50% humidity and micro-discharge disappeared completely for 12 modules up to 500 V. The suppression of the micro-discharge in humid condition can be explained by the fact that the sensor surface should become more conductive at higher humidity, which acts to reduce the charge multiplication associated to the micro-discharge process. Second, we studied the temperature dependence, comparing the *IV* curves of six micro-discharge modules at 15 and 25 °C with all at 0% humidity. The bulk leakage current should increase to 2.4 times with this temperature increase. The micro-discharge leakage current, however, turned out not to increase but decreased by typically 10%. The onset voltages were found not to change for these temperatures. The charge multiplication should increase at lower temperatures, since the carrier free path is increased due to less thermal disturbance. The present observation is qualitatively consistent with this expectation.

2.2. IR hot spot measurements

The IR measurement system is based on the Hamamatsu back-thinned 512×512 pixel CCD chip with C4880 controller. The device provides 16-bit imaging with a quantum efficiency of 92% at 650 nm and 10% at 1000 nm. The CCD was cooled to −55 °C by a Peltier cooler to reduce the dark current noise. The device was attached to a vertical stage in order to provide focusing on the test module, which was placed about 40 cm below. The whole setup was contained in a light-tight box.

The rms noise of the IR camera evaluated from fluctuations in background pictures was 3 electrons/pixel/s, and was negligible. Although negligible on average, it turned out, however, that a certain noise pattern existed. The influence of this background was minimized by subtracting the module images with and without bias, both exposed for the same period.

The exposure time was up to several minutes, depending on the hot spot intensity and on the lens magnification. The module bias was adjusted so that the leakage current was in the range of a few μA. With the wide-angle lens, the optimum exposure time was 1 min for ∼3 μA leakage and 5 min for ∼1 μA leakage. With the microscope lens, the exposure time was around 30 s.

The hot spot search started using the wide-angle lens which covered an area of half of one side of the module. The micro-discharge module was therefore exposed four times (two/side) to survey the hot spots. The hybrid [5], 2.1 cm wide, bridges across the module without touching the sensor surface nearly at the middle of the module.

This hides the sensor surface and the corresponding area, 16% of the whole, could not be surveyed. All the bonding pads, however, were fully exposed. Once a hot spot, bright spot only for the on-bias module image, is detected, the detailed position was determined using a microscope lens. The most expanded image covered a square of about 600 μm. The hot spot position was first transferred to an image taken by the same IR camera under some room light. Any visible traces were then examined with a conventional microscope. Since the position transfer is not easy in the expanded uniform image unless some characteristic pattern is detected at or near the hot spot, the characterization with conventional microscope fails if there is no such pattern in the image taken by the IR camera.

3. Results

3.1. Micro-discharge onset voltage

The *IV* curves of the first 200 modules are shown in Fig. 1. Most of the modules showed the pattern (A) where the leakage current increased rapidly up to the full depletion voltage ranged between 50 and 90 V, and then increased slowly up to 500 V. The micro-discharge onset voltage of pattern (B) was defined as the lowest voltage which deviated from the smooth curve of pattern (A). The voltage was unambiguously determined except for six modules where the current increased monotonically starting below the full depletion voltage, pattern (C). An onset voltage of a few 10 V was assigned for these modules. The total number of micro-discharge modules we identified is 111 out of 981 tested. Fig. 2 histograms the onset voltages of these modules. Among these, 80 (72%) modules have the onset voltage above 400 V, 23 (21%) modules between 200 and 400 V, and 8 (7%) modules below 200 V.

3.2. IR hot spot results

Out of the 111 micro-discharge modules, we succeeded in identifying hot spots in 61 (55%) modules. Some modules showed multiple hot spots in different sensors. They were counted separately: the number of hot spots was 72 in total.

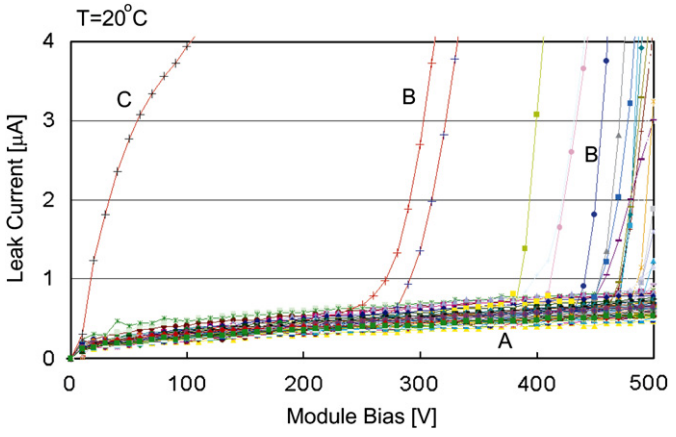

Fig. 1. *IV* curves of Module 1–200. The leakage current is normalized to 20 °C.

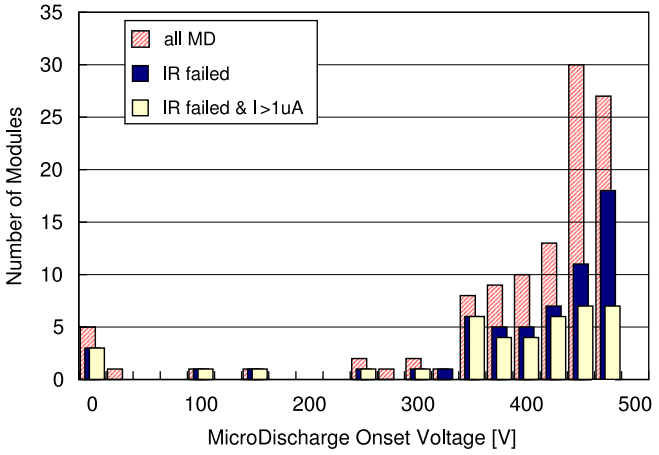

Fig. 2. The micro-discharge onset voltages for all 111 modules. The subset for 50 modules whose hot spots are not identified by IR camera are shown in dark histogram. Among 50, the leakage is greater than 1 μA for 31 modules, shown in open histogram.

Table 1
Classification of hot spot images

Number of micro-discharge modules	111	
Number of modules with hot spot identified	61	
Number of hot spots		(72)
(O) Obvious damage by mis-handling	2	(2)
(A) Implant is irregularly shaped	7	(13)
(B) Scratch-like trace underneath Al	7	(7)
(C) Cluster of dots along Al edge	5	(6)
(D) Dots in oxide/nitride layer	22	(24)
(E) No visible trace is identified	8	(8)
(F) Some trace (not classified)	3	(3)
(G) No obvious trace (not classified)	9	(9)
Hot spots at the strip edges	58	(67)
Hot spots at the bias-ring	2	(2)
Hot spots at the bonding pad edges	3	(3)

Since multiple hot spots are identified in a module, numbers in terms of hot spots are given in parentheses in addition to the numbers in terms of modules. (The number of modules totals 63 for 61 modules with identified hot sopts, since two modules can be classified into two different categories.)

Table 1 lists the numbers of 72 hot spots (61 modules) classified based on the types of traces and the locations. The two modules in type (O) have been damaged and the traces are obvious. The remainder of the 70 identified hot spots are located mostly near the strip edges: only two were found around the bias-ring edge and three around the wirebonding pad edge. In all cases, the hot spots are located at the structure edges where the electric field is largest.

Photographs of typical hot spot types are shown in Fig. 3. In type (A), the hot spot is located at the sharp edge of the irregularly shaped p^+ implant. Such irregularity was

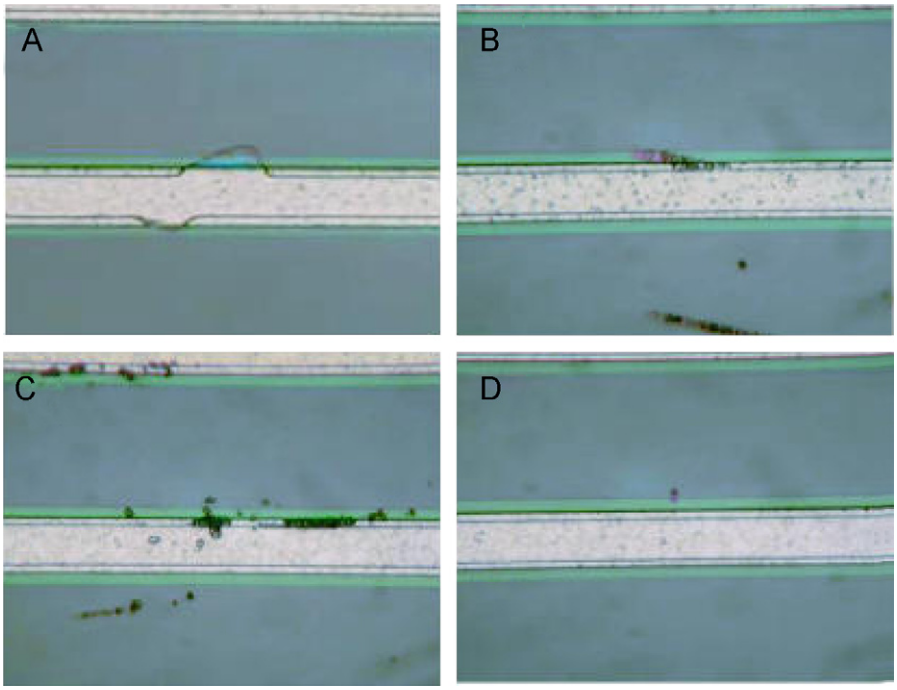

Fig. 3. Four typical types of hot spot sources. The sources are located at the center of each photo. The horizontal white strip is the Al electrode. The parallel two lines inside Al show the boundary of the p^+ implant underneath. (A) The implant is irregularly shaped; (B) scratch-like traces traversing underneath the Al strips (another trace is visible at the bottom); (C) clusters of dots are located along the Al edge; (D) a dot (or clusters of dots) is visible in oxide/nitride layer apart from the Al.

caused by improper lithography for the ion implantation. Type (B) has scratch-like irregularities running underneath the Al strip. Such scratches were created during depositions of oxide or nitride layers. Type (C) shows a cluster of dots along the Al strip edge. The Al strip edges are clear, meaning that Al deposition was done properly but rinsing was not sufficient. Although the visible anomaly is not spectacular for type (D), some colored dots are seen in the oxide/nitride layers, a few μm away from the Al strip edge. The dots should be created by droplets of photoresist resin. Eight modules (7%), type (E), show no irregular trace at the hot spot. The defects must be hidden underneath Al electrodes.

The above classification is based on the images of the conventional microscope, because the IR images are not distinct enough to perform detailed classification. In taking conventional images, we relied on a characteristic pattern close to the hot spot position to localize it. In type (G), no characteristic pattern was found in the IR image. In type (F), we found some traces in the IR image but did not continue further classification based on conventional images as was scheduled for shipping.

Excluding the two type (O) modules, the others have problems originating from processing faults, 41 modules (Types (A)–(D)) with clear traces of flaw, and 20 modules (Types (E)–(G)) without.

Among the 50 modules without identified hot sopts, four have been damaged during module fabrication and testing. Adding the two modules of type (O), the number of damaged modules thus totals to six. The leakage current for 19 modules did not exceed 1 μA, and in this case the hot spot was too tiny to detect. In fact the onset voltages for these are distributed mostly just under 500 V. Fig. 2 details the onset voltages of 50 modules without identified hot spots.

The remaining 27 modules had a large leakage exceeding 1 μA, while the hot spot was not identified. We categorize these as ''Dark'' modules. The distribution of micro-discharge onset voltages for the ''Dark'' modules is similar to the rest, as shown in Fig. 2. Taking into account the area hidden by the hybrid, some 10 modules could be explained by the hot spots being located behind the hybrid: Some 17 modules remain to be explained why the hot spot is not visible.

Among the six modules with very small onset voltage (<20 V), five modules have been damaged during module fabrication or testing, including the two type (O) modules. Only one undamaged module has ~60 μm long corrosion-like dots along the strip (see Fig. 3c), and the hot spot was identified in this location.

3.3. Micro-discharge history in the test sequence

The micro-discharge could potentially be created in many handling processes involved in the module production and testing. Actually, we almost eliminated the procedure where the sensor strip side was touched directly. The sensors were slid onto the alignment tables [6] with the strip side up, avoiding use of vacuum tweezers. When the aligned sensors were transferred to the gluing jig, the strip

side was vacuum chucked through porous paper. No glue was applied on the sensor strip side. Finally, the only jig that touched the strip face was the wire bonding head.

The completed module was kept in an aluminum box for protection. For metrology measurement, the modules needed to be transferred to another frame. Unfortunately a couple of modules were damaged by accident during this procedure creating obvious scratches on the surface.

Fig. 4 shows the evolution of the number of micro-discharge modules counted at the tests in sequence. The test sequence [1] consists of five steps, "sensor", "module", "LT", "LTL" and "final". Brief descriptions of the tests, and the temperature and humidity conditions are described in the figure caption. Among the 111 micro-discharge modules, 71 modules were fully tested in the specified sequence: the rest were not IV tested on individual sensor up to 500 V, or the tests were swapped in sequence. The evolutions are shown separately for all of these modules, 32 modules (among the 71 modules) whose hot spots were not identified, and 24 modules (among the 32 modules) with leakage larger than 1 μA ("Dark" modules). In the chart, the modules where micro-discharge is already seen in the previous test, or observed for the first time, are grouped, and the same fill patterns show the evolution of these numbers. For example in the chart (a), 14 modules are new at "LT", while 31 are since "module" and 21 are since "sensor".

The first test "sensor" is not on the modules but on individual sensors. There are 74 modules that are assembled using at least one micro-discharge sensor. Among this, 22 modules showed micro-discharge in the later tests, and 52 did not show any since assembled. These 52 modules are not categorized as micro-discharge, which are shown in dashed lines. The reduction from 74 to 22 can be explained qualitatively by the fact that bonding the Al electrodes to the ASIC inputs stabilizes the electric field and suppresses the micro-discharge development due to the overhang electrode design.

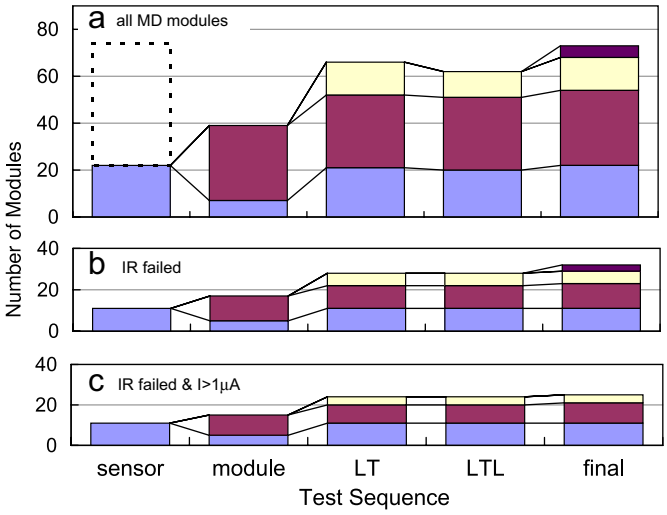

Fig. 4. The number of micro-discharge modules counted at each test in sequence. The test "sensor" is for individual sensor *IV* made prior to assembling into modules (25 °C and 50% relative humidity), "module" is the test at the module assembly sites (15 °C and 50%), "LT" (15 °C and 0%, 20 h long-term stability test), "LTL" (−16 °C and 0%, low temperature test), and "final" (15 °C and 0%, before shipping) are the tests done at KEK. (a) Seventy-one micro-discharge modules tested in the specified sequence. (b) Subset of (a) with IR hot spot not identified. (c) Subset of (b) with the leakage larger than 1 μA.

The identified micro-discharge modules are not identical at each test. This is because the onset voltages fluctuate when the test is repeated. In this view, the numbers at "LT", "LTL" and "final" can be considered equal. From "module" to "LT", the number since "sensor" increased from 7 to 21, which can be qualitatively explained by the humidity change from 50% to 0%.

Among the 32 modules new at "module", 20 modules showed IR hot spots: the problems originating in the sensor process are evident. We conclude that the sensor micro-discharge developed in this period as a result of repeated biasing or some changes created on the sensor surface. We note that the numbers did not change further in the later tests in sequence.

3.4. Micro-discharge decay time

The local high electric field responsible for the micro-discharge has a tendency to weaken with time. The SCT group has specified to evaluate the leakage current decay time by keeping 500 V bias for 24 h. The leakage current decay appears to follow an exponential function approaching an asymptotic value for most of the modules. The decay time constant is defined as the time constant of the exponential.

The time constants are plotted against the initial leakage current in Fig. 5. The modules with identified hot-spots are marked with crosses in the figure. We notice a general tendency that longer decay times are associated to larger initial leakage. There are exceptions, though, that have a long decay time (>∼1 h) irrespective of the initial leakage, and the probability of finding "Dark" modules is larger in

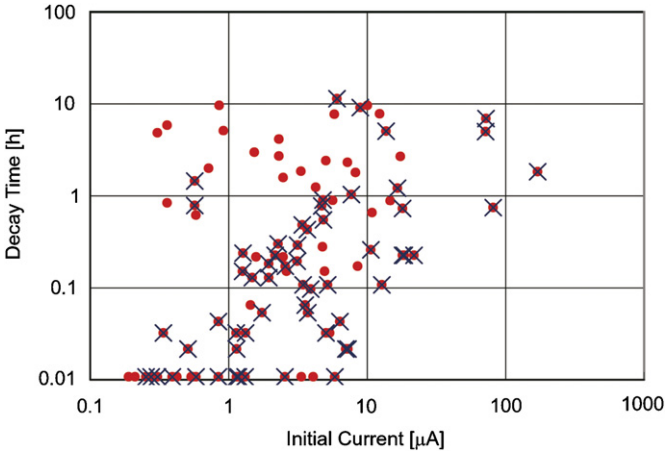

Fig. 5. The correlation between the current decay time constants and the initial leakage current, measured for 108 modules. Crosses are attached to the 61 modules whose hot spots were identified.

this group. This observation is reasonable since instantaneous hot spot intensity should be smaller for the modules with a longer decay time.

Although the reason for the "Dark" modules is not fully understood, they are probably common micro-discharge modules, but their leakage current decay time is longer. No anomaly is found in their noise distributions and history in the test sequence. The reason for the longer decay is investigated from the modules with identified hot spots and longer decay time. For these modules, no flaw associated to the hot sopts is observed, or the defects appear less severe (an example is Fig. 3d). The defects may exist inside the structures and the time to weaken the electric field takes longer.

3.5. Installation to the SCT barrels

The fact that the micro-discharge decays with time led us to install those modules subject to the onset voltage and the decay constant within predefined values. The SCT group decided to place micro-discharge modules on the outer barrels where the radiation environment is less severe and the operation voltage will be kept moderate. Following the criteria [1], 97 micro-discharge modules have been shipped for assembling into the barrels: 83 modules (with micro-discharge onset voltage $V_{MD} > 350\,V$ and the leakage decay time $T_{MD} < 1\,h$) are for the outer third or fourth barrels. Fourteen modules with $150 < V_{MD} < 350\,V$ and $T_{MD} < 6\,h$ are kept as spares. The remaining 14 modules are regarded as failed and will not be used.

4. Summary

The ATLAS Japan SCT Group has completed production of 981 barrel modules, among which 111 modules were found to show a rapid increase of leakage current at a bias below 500 V at least once in the series of the quality assurance tests. Among these 111 modules, six have been damaged in module handling. Investigation through IR hot spot imaging was successful for 61 modules in total. About 2/3 of them have evident problems in the sensor, related to photoresist processing and cleaning. The remaining 1/3 must also have problems originating in sensors but the IR hot spot could not be associated with a clear visible flaw.

Among the 50 modules for which we failed to identify any IR hot spot, 2/5 were associated with tiny micro-discharges having an onset close to 500 V. The remainder have a noise distribution consistent with that of IR luminous modules but tend to have a longer leakage current decay constant.

References

[1] A. Abdesselam, et al., Nucl. Instr. and Meth. A 568 (2006) 642.
[2] W. Dabrowski, et al., IEEE Trans. Nucl. Sci. NS-47 (2000) 382.
[3] T. Ohsugi, et al., Nucl. Instr. and Meth. A 342 (1994) 22.
[4] T. Akimoto, et al., IEEE Trans. Nucl. Sci. NS-51 (2004) 1546.
[5] Y. Unno, et al., Nucl. Instr. and Meth. A 541 (2005) 286.
[6] Y. Kato, et al., Nucl. Instr. and Meth. A 511 (2003) 132.